

Cite this: *Food Funct.*, 2022, **13**, 10601

## Steering protein and lipid digestibility by oleogelation with protein aerogels

Stella Plazzotta,<sup>1</sup> Marilisa Alongi,<sup>1</sup> Lorenzo De Berardinis, Sofia Melchior,<sup>1</sup> Sonia Calligaris<sup>1</sup>\* and Lara Manzocco

The aim of the present work was to assess the effect of an innovative oleogelation strategy, the aerogel-template approach, on protein and lipid digestibility. Whey protein isolate (WP) was converted into aerogel particles *via* supercritical CO<sub>2</sub> drying. Oleogels were then prepared by absorption of sunflower (SO) or flaxseed (FLX) oil (80%, w/w) into the aerogel particle template and subjected to *in vitro* digestion. WP aerogel-templated oleogels showed a specific destructuring behaviour during digestion. Confocal micrographs clearly demonstrated that the original oleogel structure was lost at the gastric level, with the release of oil droplets smaller ( $D_{32} < 10 \mu\text{m}$ ) than those observed in the case of the unstructured oils ( $D_{32} > 30 \mu\text{m}$ ), stabilised by undigested aerogel proteins. Sodium dodecyl sulphate polyacrylamide gel electrophoresis (SDS-PAGE) and bicinchoninic acid (BCA) assay confirmed that aerogelation reduced the gastric proteolysis of WP from nearly 100% to 70%. The digestion of the SO oleogel led to similar gastric protein digestibility. In contrast, in the case of the FLX oleogel, gastric proteolysis decreased to 40%, suggesting a role of the oil nature in steering WP aerogel digestion. In all cases, upon intestinal digestion aerogel proteins resulted completely hydrolysed. The lipolysis degree of SO (75%) and FLX (34%) oil in the oleogels was higher than that of the unstructured SO (66%) and FLX (24%) oils, due to the larger surface offered by smaller oil droplets to the action of intestinal lipases. This was confirmed by dynamic light scattering, showing a shift towards smaller size in the digestive micelle distribution of oleogels at the end of the intestinal phase. Oleogelation through the WP aerogel-template approach could be regarded as a strategy to steer lipid digestibility while also modulating the release of bioaccessible peptides.

Received 9th May 2022,  
Accepted 5th September 2022

DOI: 10.1039/d2fo01257j

rsc.li/food-function

## 1 Introduction

The growing incidence of diet-related diseases has fostered the research of strategies to increase the health profile of foods. One of the most timely strategies in the development of healthier food is the design of food architectures steering the destructuring behaviour of the matrix during digestion, and thus the release and absorption of nutrients.

Among innovative food structures, aerogels are a special type of food-grade nanostructured material, characterised by high porosity, extremely low density, and a huge internal surface.<sup>1</sup> These features make aerogels perfect candidates for the engineering of ingredients able to load high amounts of gaseous or liquid molecules. In particular, liquid edible oils can be loaded into protein aerogels in amounts ranging from 0.2 to 5.6 g oil per g aerogel, depending on the loading procedure.<sup>2,3</sup>

Making a protein aerogel starts with the preparation of an aqueous gel (hydrogel), commonly obtained by heat-induced gelation of a protein aqueous solution, which causes protein unfolding and subsequent aggregation, due to the exposure of sulfhydryl and hydrophobic groups. In the following preparation step, water in the hydrogel is dried by freeze-drying or supercritical CO<sub>2</sub> drying.<sup>4,5</sup> In the case of supercritical CO<sub>2</sub> drying, hydrogel water is substituted with ethanol, which is then removed from the polymeric network by a continuous flow of CO<sub>2</sub> in the supercritical state, leading to a porous template.<sup>3</sup> Oil absorption into whey protein (WP) aerogel particles by simple mixing seems particularly promising for food applications. In our previous work, this easy loading procedure was used to produce oleogels, *i.e.*, gels entrapping large amounts of liquid oil.<sup>6,7</sup> The obtained oleogels contained 80% oil and had a structure similar to that of traditional hard fats, thus showing high potential as innovative ingredients for the production of low-saturated fat foods. Such behaviour was attributed to the ability of WP aerogel particles to entrap the oil through different mechanisms: the oil was not only absorbed into the pores driven by capillary forces,

Department of Agricultural, Food, Environmental and Animal Sciences, University of Udine, Udine, Italy. E-mail: sonia.calligaris@uniud.it



but also immobilized in the spaces among the particles, leading to a deformable network based on weak hydrophilic interactions.<sup>6</sup>

Recent findings have demonstrated that oleogelation can be exploited to steer lipid digestibility.<sup>8–12</sup> The latter mainly occurs at the intestinal level, where the lipids are emulsified by the action of bile salts, thus facilitating the hydrolytic activity of lipases. The released free fatty acids are then included in mixed micelles and subsequently absorbed by the duodenal enterocytes.<sup>13</sup> When oleogels were obtained by oil structuring with lipid-soluble gelators (*e.g.*, waxes, monoglycerides, phytosterols, ethylcellulose) a decrease of lipid digestibility was observed as compared to those from unstructured oil.<sup>8–12</sup> Lipolysis reduction was attributed to the ability of the gelator network to hinder the access of lipolytic enzymes to the substrate. Lipolysis was shown to depend on oleogel structure. In particular, lipolysis decreased with the increase in oleogel structuration.<sup>12</sup>

By contrast, no indication is currently reported in the literature about lipolysis of oleogels obtained *via* the protein aerogel-template approach. A few studies can be cited from the literature with information relevant to the study of lipolysis in complex protein matrices containing oil. In this regard, opposite effects have been reported depending on the matrix structure and protein physical state. In oil-in-water emulsions stabilized by WPs, an increase in lipolysis kinetics and ratio was observed as compared to non-emulsified oil, thanks to the formation of small droplets offering a larger interfacial area available for lipase adsorption.<sup>14–16</sup> However, when the WPs in the emulsion continuous phase were gelled, a significant lipolysis reduction was observed, due to the ability of the protein network to reach the intestinal environment being only partially digested, thus sterically hindering lipase action.<sup>14</sup> Similarly, aerogelation resulted in the increase of WP gastric resistance, which has been exploited in the engineering of aerogel-based delivery systems, able to protect the loaded compounds through the harsh gastric environment.<sup>2</sup> Such aerogel resistance was attributed to the modifications suffered by the proteins during the different steps of the aerogel preparation, leading to a complex protein network, which hinders the action of gastric pepsin.<sup>2</sup>

This study aims at assessing the effect of the complex structure of oleogels obtained through the aerogel template approach on the digestibility of the loaded lipids and of the aerogel proteins. For this purpose, the gastrointestinal digestion of oleogels obtained by the absorption of edible oils into WP aerogel particles was simulated through an *in vitro* protocol and compared to that of the unstructured oils by determining the free fatty acid release. Sunflower (SO) and flaxseed (FLX) oils were used as loading target oils, the former being widely used in the food sector and the latter having an interesting fatty acid profile, rich in omega-3 fatty acids.<sup>17</sup> The hydrolysis of the protein aerogel template was also assessed to have an insight into the effect of aerogelation on protein digestibility.

## 2 Material and methods

### 2.1 Materials

Whey protein isolate (WP, 94.7% protein content; 74.6%  $\beta$ -lactoglobulin, 23.8%  $\alpha$ -lactalbumin, and 1.6% bovine serum albumin) was purchased from Davisco Food International Inc. (Le Sueur, MN, USA). Flaxseed (FLX) and sunflower (SO) oils were purchased in a local market. CO<sub>2</sub> (purity, 99.995%) was purchased from Sapio (Monza, Italy). P<sub>2</sub>O<sub>5</sub> was purchased from Chem-Lab NV (Zedelgem, Belgium). Agar technical (Agar No. 3) was purchased from Oxoid Limited (Basingstoke, UK). Fast Green FCF and Nile Red dyes, porcine pepsin, porcine lipase, porcine pancreatin (8 $\times$  USP), porcine bile extract, HCl, NaOH, CaCl<sub>2</sub>, Na<sub>2</sub>CO<sub>3</sub>, NaCl, KCl, KH<sub>2</sub>PO<sub>4</sub>, MgCl<sub>2</sub>(H<sub>2</sub>O)<sub>6</sub>, (NH<sub>4</sub>)<sub>2</sub>CO<sub>3</sub>, MgSO<sub>4</sub>, Tris-HCl, SDS, bicinchoninic acid solution, cupric sulphate solution, acetic acid, Tris base, sodium dodecyl sulfate (SDS), glycine, and bovine serum albumin (BSA) were purchased from Sigma Aldrich (Milan, Italy). Absolute ethanol and methanol were purchased from J.T. Baker (Griesheim, Germany). Laemmli sample buffer 2 $\times$ ,  $\beta$ -mercaptoethanol, Mini-PROTEAN® TGX Stain-Free™ precast gels, Bio-Safe™ Coomassie G-250 stain, and the protein standards for SDS-PAGE (Precision Plus Protein Standards, Kaleidoscope) were purchased from Bio-Rad Laboratories Inc. (Hercules, California, USA). Deionized water (System Advantage A10®, Millipore S.A.S., Molsheim, France) was used for all the analyses.

### 2.2 Oleogel preparation

WP aerogel particles were prepared as previously described.<sup>6</sup> Briefly, WP aqueous solutions (20%, w/w) were adjusted at pH 5.7 and gelled at 85 °C for 15 min in sealed 50 mL plastic tubes. The obtained hydrogel was cooled and homogenized using a high-speed mixer at 13 000 rpm for 3 min (Polytron PT-MR3000, Kinematica AG, Littau, Switzerland). The hydrogel particles were then dispersed in ethanol (0.1 g mL<sup>-1</sup>), homogenized and collected by centrifugation at 13 000g for 10 min at 4 °C (Avanti J-25, Beckman, Palo Alto, CA, USA). This procedure was repeated twice to completely remove water. The ethanol was then removed using a supercritical CO<sub>2</sub>-drying plant at 60 °C and 120 bar. The obtained dried aerogel particles were refined by grinding for 1 min using a domestic grinder (MC3001, Moulinex, Milan, Italy). The powder was then dispersed into oil (0.1 g mL<sup>-1</sup>) and homogenized at 13 000 rpm for 3 min. The oil-absorbed particles were collected by centrifugation, as previously described. The collected particles were re-dispersed in oil (0.1 g mL<sup>-1</sup>) and centrifuged, obtaining oleogels presenting 80% (w/w) oil content, whose complete characterization has been previously reported.<sup>6,7</sup>

### 2.3 Powder solubility

The solubility of WP isolate and aerogel particles was assessed gravimetrically as reported by Melchior *et al.*<sup>18</sup> Three aliquots of WP isolate or aerogel powder (*W*<sub>0</sub>, 100 mg) were suspended in 1 mL of deionized water (pH = 7.0  $\pm$  0.2) and stirred for 2 min at 37 °C. One aliquot was centrifuged at 15 000g for



5 min at 4 °C (D3024, DLAB Scientific Europe S.A.S., Schiltigheim, France). The supernatant and the precipitate were carefully separated. The insoluble precipitates were dried in a vacuum oven at 75 °C overnight (Vuotomatic 50, Bicasa, Milan, Italy) and weighed ( $W_1$ , mg). Powder solubility was expressed according to eqn (1):

$$\text{Powder solubility (\%)} = \frac{W_0 - W_1}{W_0} \times 100. \quad (1)$$

The second and third aliquots were adjusted to pH 3.0 with HCl 1 M and stirred at 37 °C for 2 h. The solubility of the second aliquot was then determined; the third aliquot was adjusted to pH 8.0 with NaOH 1 M, further stirred at 37 °C for 2 h, and finally assessed for solubility.

#### 2.4 *In vitro* digestion

*In vitro* digestion was carried out according to the INFOGEST static digestion protocol proposed by Brodkorb *et al.*<sup>19</sup> Briefly, the simulated salivary (SSF), gastric (SGF) and intestinal (SIF) fluids were prepared, stored at 4 °C and preheated to 37 °C just before *in vitro* digestion. Amyolytic enzymes were not considered due to the lack of carbohydrates in the digested matrices. The oral phase was started by adding to the sample 4 mL of SSF, 25 µL of 0.3 M CaCl<sub>2</sub>, and 975 µL of water. The sample was maintained at 37 °C under stirring for 2 min. At the end of the oral phase, 8 mL of SGF, 5 µL of 0.3 M CaCl<sub>2</sub>, and 667 µL of aqueous pepsin solution providing 2000 U mL<sup>-1</sup> activity in the final chyme, were added. To start the gastric phase, pH was adjusted to 3.0 with 1 M HCl and the volume was made up to 20 mL with water. The mix was stirred at 37 °C for up to 2 h. At the end of the gastric phase, 8 mL of SIF, 4 µL of 0.3 M CaCl<sub>2</sub>, 5 mL of a lipase–pancreatin solution, prepared in SIF and providing 2000 and 100 U mL<sup>-1</sup> activity respectively in the final mixture, and 3 mL of 160 mM bile extract prepared in SIF were added. To start the intestinal phase, pH was adjusted to 8.00 ± 0.10 with 1 M NaOH and the volume was made up to 40 mL with water. The mix was stirred at 37 °C for up to 2 h.

#### 2.5 Confocal microscopy

A 0.2% aqueous solution of Fast Green and Nile Red was used to stain, respectively, the proteins and the oil. The hanging-drop method was used<sup>20</sup> to analyze the samples collected after the gastric and intestinal digestion phases. After staining, agarose (1%, w/w) was added to the samples in a sample : agarose ratio of 1 : 2 (v/v). An amount of 2 µL of the obtained mix was placed on a microscope cover-slip and left to set for 1 min. The cover-slip with the gelled droplet was then fixed on a concave microscope slide and observed using a confocal laser scanning microscope at 100× magnification (Leica TCS SP8 X confocal system, Leica Microsystems, Wetzlar, Germany). Images were imported in the jpeg format using the software LasX 3.5.5 (Leica Microsystems, Wetzlar, Germany). Oil droplet dimension was determined based on the image analysis of confocal micrographs using Image-Pro Plus 6.3 (Media Cybernetics Inc., USA). Images were converted to 8-bit

grey scale and software calibration was applied. Droplet diameter data were provided by the software and further elaborated to obtain the  $D_{32}$  (Microsoft® Excel®).

#### 2.6 Protein digestibility

Protein digestibility trials were conducted on 0.25 g WP aerogel particles and native WP (used as the control), as well as on the WP aerogel templated oleogels. At the end of the gastric and intestinal phases, hydrolysis was stopped by adding ethanol (1 : 3, v/v). Samples were then centrifuged with a high-speed centrifuge (Avanti Centrifuge™ J-25, Beckman Coulter, Indianapolis, IN, USA) at 11 000g for 10 min at 4 °C. The supernatant and the precipitate were separated, and the precipitate (undigested fraction) was freeze-dried (Epsilon 2-4 LSCplus, Martin Christ GmbH, Osterode am Harz, Germany), and stored in a desiccator containing P<sub>2</sub>O<sub>5</sub> at room temperature until use.

**2.6.1 Sodium dodecyl sulphate polyacrylamide gel electrophoresis (SDS-PAGE).** SDS-PAGE was performed according to the method of Laemmli.<sup>21</sup> An amount of dried precipitate containing 3 mg of proteins (based on BCA assay, Section 2.6.2) was mixed with 500 µL of Laemmli sample buffer 2× in the presence of 10 µL of the reducing agent β-mercaptoethanol, incubated for 1 h at 20 °C, heated at 95 °C for 5 min, and centrifuged for 10 min at 10 000g at 20 °C (Mikro 120, Hettich Italia S.r.l., Milan, Italy). Then, 10 µL of the prepared sample was loaded into SDS-PAGE pre-stained gels (Mini-PROTEAN TGX Stain-Free Gels, Bio-Rad Laboratories, Inc., Hercules, CA, USA) and the electrophoresis was performed at 30 mA (Mini-PROTEAN® Tetra Cell apparatus, Bio-Rad, Hercules, CA, USA). The running buffer was made of 1.92 M glycine, 250 mM Tris base, and 1% SDS. Gels were then placed for 30 min in a gel-fixing solution (40% methanol and 10% acetic acid) and stained with Coomassie blue overnight. A bioanalytical imaging system (G:Box Chemi XX9, Syngene, Cambridge, UK) was used to see the protein lanes and the software GeneSys (Syngene, Cambridge, UK) was used to take the gel images. Protein identification was based on the comparison with protein standards in the molecular weight range 10–250 kDa.

**2.6.2 Bicinchoninic acid (BCA) assay.** The protein content in the dried precipitate was quantified by BCA assay according to Smith *et al.*,<sup>22</sup> adapted to a 96-well microplate spectrophotometer procedure. This assay is based on the reaction of peptides containing three or more amino acid residues with cupric ions to form a colored chelate complex, and spectrophotometrically detected.<sup>23</sup> The BCA working reagent (WR) was prepared by mixing the bicinchoninic acid solution with cupric sulphate solution (4%, w/v) to reach the final ratio of 50 : 1. An extraction buffer (pH = 7.5), prepared with Tris–HCl 60 mM and SDS (2%, w/v), was used to extract proteins from the dried precipitate fraction. Samples were diluted with water to reach the final concentration within the range of the calibration curve, and were prepared using bovine serum albumin (0–2000 µg mL<sup>-1</sup> bovine serum albumin,  $R^2 = 0.994$ ). Aliquots of 25 µL of diluted samples were placed into a 96-well Microtiter™ microplates (Thermo Fisher Scientific, Waltham,



MA, USA) and 200  $\mu\text{L}$  of WR was added to each well. Samples were incubated in a microplate reader (Sunrise-Basic Tecan, Tecan GmbH, Grödig, Austria) at 37 °C for 30 min in the dark. Then the absorbance was measured at 562 nm and protein content ( $P$ ,  $\mu\text{g mL}^{-1}$ ) determined by comparison with the calibration curve. Digested proteins, *i.e.*, free amino acids and dipeptides, were computed by eqn (2):

$$\text{Digested proteins (\%)} = \frac{P_0 - P_1}{P_0} \times 100 \quad (2)$$

where  $P_0$  is the protein content in the blank (undigested sample) and  $P_1$  is the protein content detected in the precipitate obtained after each digestion phase.

### 2.7 Lipid digestibility

For lipid digestibility trials,  $\text{NaHCO}_3$  was replaced with  $\text{NaCl}$  in SSF, SGF and SIF as suggested for the pH-stat approach, which was used to determine the extent of lipid digestibility.<sup>24</sup> Immediately after the addition of lipase (Section 2.4), the pH of the digestion mixture was monitored and maintained at  $8.00 \pm 0.10$  by adding 0.25 M  $\text{NaOH}$ . The choice of using pH 8.00 instead of 7.00 was based on the technical specifications of the used lipase. Based on oleogel composition (80% oil content), an oleogel amount of 1.25 g, corresponding to 1 g oil, was used, and the volume of  $\text{NaOH}$  (mL) added to titrate the oleogels was recorded ( $V_{\text{oleogel}}$ ). An aliquot of lipid-free aerogel particles (0.25 g) corresponding to that contained in the oleogels was also digested to estimate the proteolysis contribution to pH lowering and the required  $\text{NaOH}$  volume registered ( $V_{\text{aerogel}}$ ). In the case of oleogels,  $V_{\text{aerogel}}$  was multiplied by a corrective factor (% digested proteins in the oleogel/% digested proteins in the aerogel template) based on the BCA results (Section 2.6.2), to take into account the actual proteolysis under the intestinal phase.

Finally, the  $\text{NaOH}$  volume required to titrate unstructured SO and FLX oils (1 g) was also recorded ( $V_{\text{oil}}$ ).

The percentage of free fatty acids (FFA) released during lipolysis was calculated according to eqn (3):

$$\text{FFA (\%)} = \frac{V_e}{V_t} \times 100 \quad (3)$$

where  $V_e$  is the experimental volume, represented by (i)  $V_{\text{oil}}$  in the case of oils; and (ii) the difference between  $V_{\text{oleogel}}$  and  $V_{\text{aerogel}}$  in the case of oleogels, based on the assumption that proteolysis is not affected by the presence of oil, as reported in the literature studies aimed at optimizing the pH-stat approach on complex matrices containing oil and proteins.<sup>14,24</sup>  $V_t$  represents the theoretical volume required to titrate the fatty acids released by the complete hydrolysis of triglycerides in the reaction vessel, assuming 2 FFA are produced for each triacylglycerol molecule,<sup>24</sup> and was calculated according to eqn (4):

$$V_t = 2 \times \left[ \frac{m_{\text{oil}}}{\text{MW}_{\text{oil}}} \frac{1000}{C_{\text{NaOH}}} \right] \quad (4)$$

where  $m_{\text{oil}}$  is the mass of oil in the reaction vessel (g),  $\text{MW}_{\text{oil}}$  is the average molecular weight of SO (876.6  $\text{g mol}^{-1}$ ) and FLX

(542.6  $\text{g mol}^{-1}$ ) oils and  $C_{\text{NaOH}}$  is the concentration of sodium hydroxide (M). The maximum value of FFA released during digestion was determined after the plateau was reached, *i.e.*, after 30 min from the beginning of the intestinal phase. This value was considered as an indication of the maximum lipolysis and was reported as  $\text{FFA}_{\text{max}}$ .

### 2.8 Micelle size distribution

Digestate samples were collected at the end of the intestinal phase. The enzymatic hydrolysis was stopped by adding ethanol (sample : ethanol = 1 : 3, v/v). Samples were then centrifuged with a high-speed centrifuge (Avanti Centrifuge™ J-25, Beckman Coulter, Indianapolis, IN, USA) at 30 000g for 70 min at 4 °C. The supernatant was collected and immediately analyzed. The particle size distribution was measured by dynamic laser light scattering (DLS, Zetasizer NanoZS, Malvern Instruments, Worcestershire, UK). Samples were poured in plastic cuvettes, placed in the instrument cell and analyzed at 25 °C. The angle of observation was 173°. The solution refractive index and viscosity were set at 1.333 and 0.001 Pa s, corresponding to the values of pure water at 25 °C. The particle mean diameter corresponding to volume distribution was calculated by distribution analysis fitting.

### 2.9 Data analysis

The results determined were expressed as the mean  $\pm$  standard deviation of at least three repeated measurements from two experiment replicates. Statistical analysis was performed using R v. 3.0.2 (The R Foundation for Statistical Computing). A one-way analysis of variance (ANOVA) was carried out to identify significantly different samples ( $p < 0.05$ ).

## 3 Results and discussion

Oleogels were obtained *via* absorption into the WP aerogel particles of SO and FLX oil, as described elsewhere.<sup>6,7</sup> In particular, the oleogels presented a lipid content (80%, w/w) and a rheological behaviour ( $G' = 3.0 \times 10^5$  Pa, critical stress = 723 Pa) comparable to those of traditional hard fats (*e.g.*, margarine, butter).<sup>6</sup> The complete characterization of the oleogels is reported in our previous works.<sup>6,7</sup> The samples were *in vitro* digested to study lipid and protein digestibility. The microstructure of the digestate was first observed to gain an overall understanding of the complex interplay among protein aerogels and oil lipids under digestive conditions. Fig. 1 reports the confocal micrographs of the samples obtained after gastric and intestinal digestion of SO and FLX oil oleogels and of the corresponding unstructured oils.

Upon gastric digestion, SO and FLX oil digested samples presented large droplets with a  $D_{32}$  around 35 and 45  $\mu\text{m}$ , respectively. This was expected, due to the immiscibility of oil with the aqueous gastric environment.<sup>16,25</sup> In contrast, upon intestinal digestion, small and uniformly distributed oil droplets were observed for both SO and FLX oils, with a  $D_{32}$  of 6 and 2  $\mu\text{m}$ , respectively. This is due to the emulsifying action of



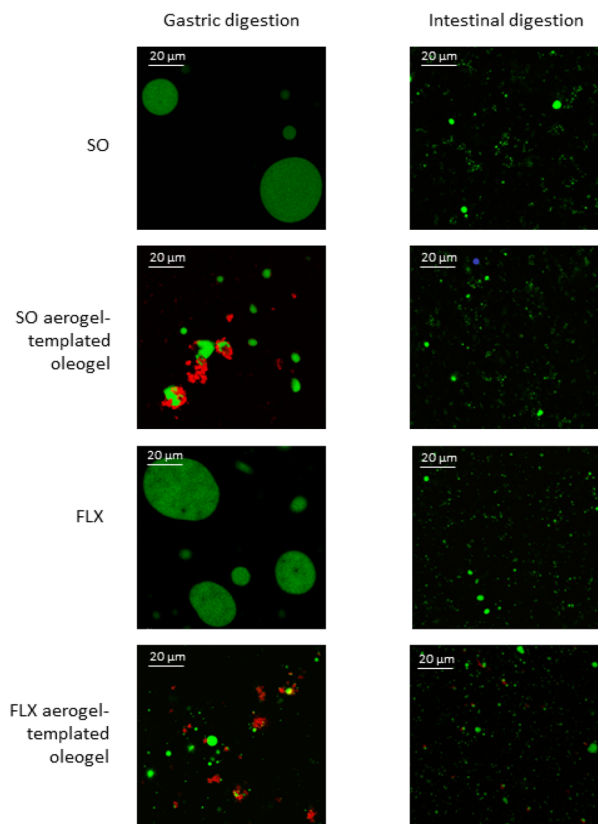


**Fig. 1** Confocal micrographs of the digestate samples obtained upon gastric and intestinal digestion of unstructured sunflower (SO) and flaxseed (FLX) oil and of the corresponding whey protein aerogel-templated oleogels. Green: oil; red: proteins.

bile salts, associated with the continuous mixing aiming at simulating peristaltic movements, which lets the large oil droplets to break into smaller ones, easily attacked by the lipases.<sup>25</sup> In the gastric environment, the initial structure of the oleogel was partly lost with the formation of oil droplets smaller than those observed for the unstructured oils, having a  $D_{32}$  around 9 µm (SO oleogel) and 4 µm (FLX oleogel) (Fig. 1). It can also be noted that many of these oil droplets were surrounded by WP aerogel particles, whose original scaffold was still clearly evident upon the gastric phase (Fig. 1). WPs have been clearly shown to position on the surface of oil droplets during digestion, due to their surface activity.<sup>14</sup> However, when WPs not submitted to aerogelation are used as emulsifiers, they generally show increased susceptibility to digestion.<sup>14</sup> This suggests that the aerogelation of proteins led to high resistance to gastric proteolysis, confirming the literature data.<sup>2</sup> Aerogel scaffolds were no more detected after the intestinal digestion, suggesting their susceptibility to intestinal proteases. Interestingly, the oil droplet distribution after the intestinal digestion of oleogels was similar to that of the unstructured oils ( $D_{32}$  of 6 µm and 3 µm for SO and FLX oleogel, respectively).

The destructuring behaviour of oleogels in the gastrointestinal environment is likely to affect the digestibility of both proteins and lipids, which was thus investigated in depth.

### 3.1 Protein digestibility in aerogels and aerogel-templated oleogels

To determine the effect of aerogelation on protein digestibility, the latter was assessed on lipid-free WP aerogels as compared to unstructured WP. Fig. 2 shows the SDS-PAGE patterns of WP and WP aerogel particles before and after gastric and intestinal digestion.

Before digestion, both samples showed the presence of typical WPs:<sup>26</sup>  $\beta$ -lactoglobulin ( $\beta$ -Lg, 18 kDa),  $\alpha$ -lactalbumin ( $\alpha$ -La, 14 kDa), lactoferrin (LF) and lactoperoxidase (LP) (75 kDa), and bovine serum albumin (BSA, 70 kDa). The absence of bands at a low molecular weight (<10 kDa) confirmed the absence of peptides before digestion. After the gastric digestion of WP, peptide bands were well evident, with the concomitant disappearance of high MW protein bands (LF, LP, BSA). Their absence clearly shows that WPs were mostly digested by gastric pepsin.<sup>27</sup> After the gastric phase,  $\beta$ -Lg and  $\alpha$ -La bands were less pronounced but still present, confirming their higher hydrolysis resistance.<sup>27</sup> Only a few peptide bands were present after the intestinal phase, indicating that most of the proteins were completely hydrolyzed to small peptides with molecular weight lower than 2 kDa. In contrast, after gastric hydrolysis of WP aerogels, the SDS-PAGE pattern showed the same protein bands of the undigested sample, even if less pronounced, along with a few peptide bands with MW in the range 2–10 kDa. This confirms that aerogelation increased protein resistance to peptic action, in agreement with the literature findings.<sup>2</sup> During the production of WP aerogel particles used in this study, insoluble structures, called microgels, are formed by thermal coagulation near the isoelectric pH.<sup>6</sup> Microgels can be attacked by pepsin only at the surface<sup>28</sup> and their aerogelation further increases the WP digestive resistance by inducing protein clustering into large

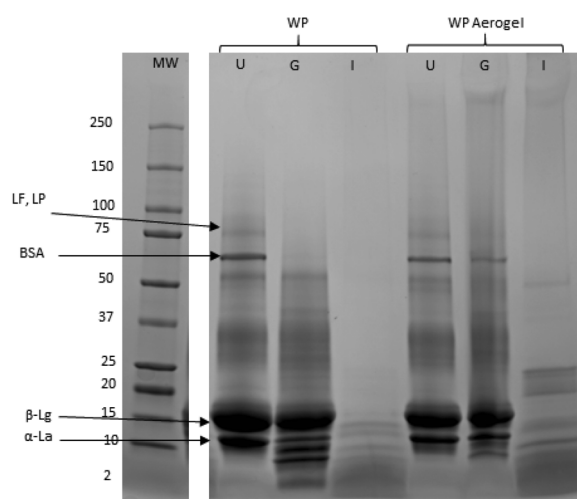


**Fig. 2** SDS-PAGE patterns of unstructured whey proteins (WP) and whey protein aerogels (WP aerogel) before (undigested, U) and after gastric (G) and intestinal (I) digestion. MW: standard molecular weights, LF: lactoferrin, LP: lactoperoxidase, BSA: bovine serum albumin,  $\alpha$ -La:  $\alpha$ -lactalbumin,  $\beta$ -Lg:  $\beta$ -lactoglobulin.



aggregates, which are probably not easily accessible to gastric enzymes.<sup>2</sup> Interestingly, low MW protein and peptide bands were detected after the intestinal digestion of WP aerogels, suggesting that the hydrolysis of the protein backbone only took place during this phase. This was initially attributed to the solubilization of the WP aerogels. However, differently from WP, which, as expected, resulted readily water-soluble under oral digestion conditions (2 min, 37 °C, pH 7.0), WP aerogels showed an oral solubility of  $9.8 \pm 3.2\%$ , which did not significantly increase even upon further exposure to gastric ( $11.0 \pm 2.2\%$ ) and intestinal ( $8.8 \pm 1.9\%$ ) conditions (2 h, 37 °C, pH 3.0 followed by 2 h, 37 °C, pH 8.0). The reduced WP aerogel solubility can be attributed to both exposure of the hydrophobic surface induced by gelation and protein aggregation induced by solvent exchange and supercritical CO<sub>2</sub> drying.<sup>29</sup> Despite the low solubility of aerogel proteins under gastrointestinal conditions, upon prolonged contact with water, they might swell and lose structural integrity,<sup>29</sup> thus becoming more susceptible to the hydrolytic activity of proteases. Moreover, it cannot be excluded that the passage from the stomach to the intestine further destabilized the compact structure of the aerogel particles, possibly due to the burst pH shift. In this regard, a significant effect of pH has been reported on the swelling and thus on the structural integrity of protein aerogels by Kleemann *et al.*<sup>2</sup> The SDS-PAGE results were confirmed by the quantification of digested proteins with BCA assay (Fig. 3).

The WP isolate was almost completely digested to dipeptides and free amino acids after the gastric phase. In contrast, about 70% of the aerogel proteins resisted gastric hydrolysis and were subsequently digested in the intestine. In other words, despite the different susceptibility of WP and WP aerogel particles to simulated gastrointestinal conditions, at the end of digestion, both samples resulted completely digested. Thus, the conversion of proteins into aerogels was

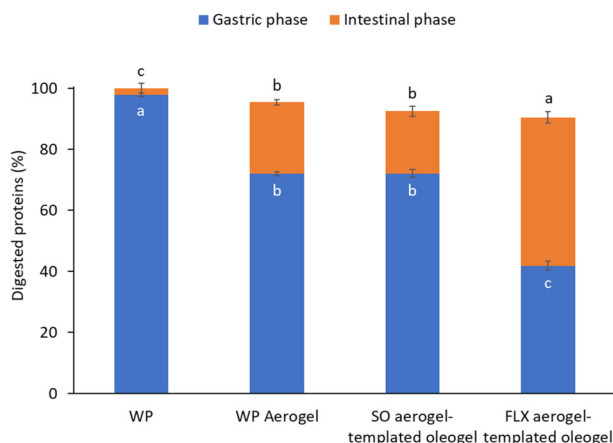


**Fig. 3** Digested proteins after gastric and intestinal digestion of unstructured whey protein (WP), whey protein aerogel particles (WP aerogel) and whey protein aerogel-templated oleogels prepared with sunflower (SO) and flaxseed (FLX) oil. <sup>a-c</sup>: For each digestion phase, means indicated by different letters are statistically different ( $p < 0.05$ ).

not found to compromise the overall bioaccessibility of proteins, *i.e.*, the fraction of small peptides and amino acids that can be absorbed through the intestinal epithelium, thus becoming available for metabolic functions.<sup>30</sup> Rather, the aerogelation process allowed for a slower and more progressive release of bioaccessible peptides, which appears interesting and valuable for further studies.

Similar protein digestion extent under gastric and intestinal conditions was observed when the aerogel was used as a template in the production of SO oleogels (Fig. 3), indicating a negligible effect of SO on the digestibility of the aerogel proteins. Conversely, FLX oil significantly reduced the susceptibility of the WP template to gastric proteolysis (Fig. 3). Despite the complex mechanisms behind the digestion of a multi-component matrix as the oleogels here considered, the higher polarity of FLX oil as compared to that of SO oil<sup>31</sup> may explain the obtained results. In particular, more polar oils have been demonstrated to form more intense interactions with dried protein particles<sup>32</sup> possibly physically hindering the access of proteases to the aerogel protein scaffold.

Nevertheless, at the end of the intestinal digestion, the aerogel proteins in the oleogels were completely digested, independently of the presence and nature of the used oil (Fig. 3), confirming the confocal microscopy data (Fig. 1). It can be assumed that upon oil digestion, occurring in the intestinal phase, oil physical hindrance was removed, resulting in the exposure of the protein particles to the action of the intestinal proteases.

### 3.2 Oil digestibility in aerogel-templated oleogels

Fig. 4 reports the percentage of free fatty acids (FFA) released during the intestinal *in vitro* digestion of SO and FLX oil oleogels and of the corresponding unstructured oils.

Typical profiles of FFA release during digestion were obtained, showing a faster rate in the first minutes followed by slower kinetics after an inflection point.<sup>14,24,33</sup> The FFA

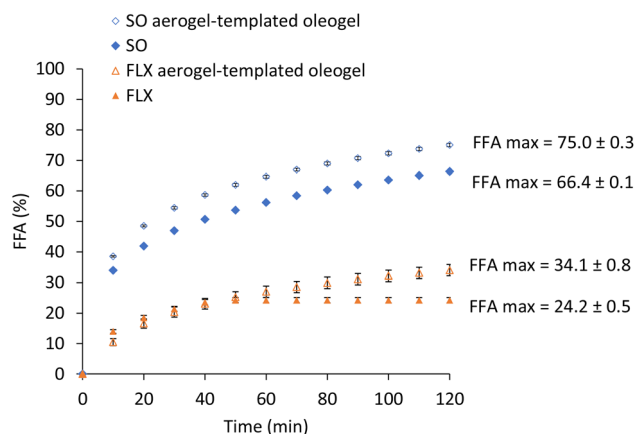


**Fig. 4** Percentage of free fatty acids released during *in vitro* intestinal digestion of unstructured sunflower (SO) and flaxseed (FLX) oils and of the corresponding whey protein aerogel-templated oleogels. Inset data reports the maximum lipolysis of the samples (FFA max).



released after 2 h intestinal digestion was used to determine the maximal lipolysis ( $\text{FFA}_{\text{max}}$ ), which yielded around 66 and 24% for SO and FLX oil, respectively. These results can be attributed to the different steric obstruction of the triglycerides of the two oils, affected by both the unsaturation degree and the average length of the fatty acid chains.<sup>10</sup> In this regard, FLX oil is rich in  $\omega$ -3 polyunsaturated fatty acids;<sup>17</sup> whereas the fatty acid composition of SO oil is mainly represented by oleic and linoleic acid, followed by palmitic acid.<sup>34</sup> Oil structuring into the WP aerogel-templates led to an increase in the lipolysis degree, with  $\text{FFA}_{\text{max}}$  values around 75 and 34% for SO and FLX oil, respectively (Fig. 4). This result was quite surprising, since the presence of a network entrapping the oil has been previously reported to have the opposite effect of reducing oil susceptibility to digestion. For example, oleogelation with waxes, phytosterols, or monoglycerides resulted in a reduced lipolysis of high oleic sunflower oil and canola oil.<sup>12,35</sup> The obtained results could be explained based on the structure of the oleogels considered in this study, and on their de-structuring behaviour during digestion. This is consistent with the results of Li *et al.*,<sup>36</sup> where the structure of oleogels from alginate-gelatine aerogels was found to affect the *in vitro* digestibility of the loaded oil.

Smaller particles (Fig. 1) would expose a larger surface for the action of lipases,<sup>33,37</sup> possibly explaining why oil structuring by aerogel particles favoured the lipolysis in the small intestine (Fig. 4). Moreover, aerogel particles were actually made of WP, which are commonly used surfactants. It cannot thus be excluded that WP aerogels acted as emulsifiers in the intestinal digestive mix, further favouring lipolysis. In this regard, a similar enhancement in lipolysis was also observed when oil was co-digested with monoglycerides, which are known to present a prominent surfactant activity.<sup>38</sup> The enhanced digestibility of the oil in the oleogel was further confirmed by analysing the dimension and distribution of digestive micelles (Fig. 5).

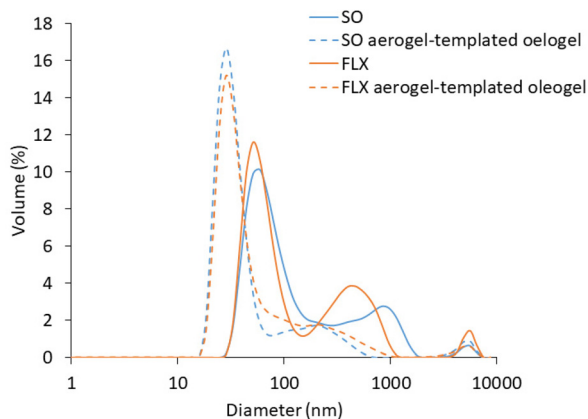


Fig. 5 Particle size distribution of micelles obtained after *in vitro* intestinal digestion of unstructured sunflower (SO) and flaxseed (FLX) oils and of the corresponding whey protein aerogel-templated oleogels.

For both SO and FLX oils, the DLS profiles of the digestate fraction containing the micelles showed a tri-modal distribution. The prominent family, with a dimension of around 60 nm, is attributable to the mixed micelles formed upon digestion and represents the fraction that can be potentially absorbed through the intestinal epithelium;<sup>39</sup> the minor particle families at 530 and 5500 nm are instead probably represented by undigested lipid droplets.<sup>40,41</sup> In the case of oleogels, a three-peak distribution was still obtained but a shift towards smaller particle dimensions, associated with an increased frequency of the smaller-dimension families, was obtained for both the considered oils. Oil structuring within WP aerogels thus resulted in a modification of micelle dimension distribution at the intestinal level (Fig. 5). Therefore, it can be inferred that WP aerogel-template oleogelation may play a role in determining the absorption of loaded lipophilic bioactive compounds. Such an effect would depend on the de-structuring behaviour of aerogel-templated oleogels, which delivered the oil in the intestine in the form of small particles surrounded and stabilized by surface active proteins, resistant to gastric digestion.

## 4 Conclusions

The destructing behaviour of WP aerogel-templated oleogels during gastro-intestinal digestion steers both proteins and oil digestibility.

Looking at protein digestibility, aerogelation increases WP gastric resistance. The latter is also influenced by the type of oil used for oleogel preparation. Nevertheless, complete protein hydrolysis is obtained after the intestinal phase, regardless of the presence and nature of the used oil.

Aerogel-template oleogelation also allows the loaded oil to be released in the small intestine in the form of a finely dispersed phase, stabilised by undigested aerogel WP proteins at the oil droplet surface. As a result, the loaded oil is more susceptible to intestinal lipolysis resulting in a higher lipid digestibility, contrary to what was generally observed when using other oil structuring agents.

The properties of aerogel-templated oleogels make them promising candidates as fat replacers able not only to provide the required technological performances but also to tune the digestibility of both the protein template and the structured oil.

From one side, this approach could be used to modulate the release, stability, and functionality of bioactive peptides derived from whey proteins. From the other, this strategy would be particularly interesting to deliver lipophilic bioactive molecules, such as polyunsaturated fatty acids here considered. Moreover, the possibility to increase lipid digestibility can represent an advantage in subjects with restrained lipid digestion, such as the elderly, who physiologically present lower lipolytic enzyme secretion, or in patients with reduced bile secretion or whose gallbladder has been removed.



## Author contributions

Conceptualization: SP, SC and LM, data curation: LDB and SM, formal analysis: SP, MA, SM and LDB, investigation: SP and LDB, methodology: SP, MA, LDB and SM, project administration: SC and LM, resources: LM, supervision: SC and LM, visualization: SP and LDB, writing – original draft: SP, writing – review and editing: all the authors.

## Conflicts of interest

There are no conflicts to declare.

## Acknowledgements

This publication is based upon work from COST Action “Advanced Engineering of aerogels for Environment and Life Sciences” (AEROGELS, ref. CA18125), supported by COST (European Cooperation in Science and Technology).

## References

- C. A. García-González and I. Smirnova, Use of supercritical fluid technology for the production of tailor-made aerogel particles for delivery systems, *J. Supercrit. Fluids*, 2013, **79**, 152–158.
- C. Kleemann, *et al.*, In-vitro-digestion and swelling kinetics of whey protein, egg white protein and sodium caseinate aerogels, *Food Hydrocolloids*, 2020, **101**, 105534.
- L. Manzocco, K. S. Mikkonen and C. A. García-González, Aerogels as porous structures for food applications: Smart ingredients and novel packaging materials, *Food Struct.*, 2021, **28**, 100188.
- M. Betz, C. A. García-González, R. P. Subrahmanyam, I. Smirnova and U. Kulozik, Preparation of novel whey protein-based aerogels as drug carriers for life science applications, *J. Supercrit. Fluids*, 2012, **72**, 111–119.
- A. Feichtinger and E. Scholten, Preparation of protein oleogels: Effect on structure and functionality, *Foods*, 2020, **9**, 1745.
- S. Plazzotta, S. Calligaris and L. Manzocco, Structural characterization of oleogels from whey protein aerogel particles, *Food Res. Int.*, 2020, **132**, 109099.
- S. Plazzotta, *et al.*, Conversion of whey protein aerogel particles into oleogels: Effect of oil type on structural features, *Polymers*, 2021, **13**, 4063.
- C. M. O'Sullivan, M. Davidovich-Pinhas, A. J. Wright, S. Barbut and A. G. Marangoni, Ethylcellulose oleogels for lipophilic bioactive delivery – effect of oleogelation on in vitro bioaccessibility and stability of beta-carotene, *Food Funct.*, 2017, **8**, 1438–1451.
- S. Y. Tan, E. Wan-Yi Peh, A. G. Marangoni and C. J. Henry, Effects of liquid oil vs. oleogel co-ingested with a carbohydrate-rich meal on human blood triglycerides, glucose, insulin and appetite, *Food Funct.*, 2017, **8**, 241–249.
- S. Y. Tan, E. Peh, P. C. Siow, A. G. Marangoni and C. J. Henry, Effects of the physical-form and the degree-of-saturation of oil on postprandial plasma triglycerides, glycemia and appetite of healthy Chinese adults, *Food Funct.*, 2017, **8**, 4433–4440.
- W. Limpimwong, T. Kumrungsee, N. Kato, N. Yanaka and M. Thongngam, Rice bran wax oleogel: A potential margarine replacement and its digestibility effect in rats fed a high-fat diet, *J. Funct. Foods*, 2017, **39**, 250–256.
- S. Calligaris, M. A. Alongi, P. Lucci and M. Anese, Effect of different oleogelators on lipolysis and curcuminoid bioaccessibility upon in vitro digestion of sunflower oil oleogels, *Food Chem.*, 2020, **314**, 126146.
- E. Bauer, S. Jakob and R. Mosenthin, Principles of physiology of lipid digestion, *Asian-Australas. J. Anim. Sci.*, 2005, **18**, 282–295.
- D. J. L. Mat, I. Souchon, C. Michon and S. Le Feunteun, Gastro-intestinal in vitro digestions of protein emulsions monitored by pH-stat: Influence of structural properties and interplay between proteolysis and lipolysis, *Food Chem.*, 2020, **311**, 125946.
- D. J. McClements and Y. Li, Structured emulsion-based delivery systems: Controlling the digestion and release of lipophilic food components, *Adv. Colloid Interface Sci.*, 2010, **159**, 213–228.
- M. Armand, *et al.*, Characterization of emulsions and lipolysis of dietary lipids in the human stomach, *Am. J. Physiol.: Gastrointest. Liver Physiol.*, 1994, **266**, 372–381.
- A. Goyal, V. Sharma, N. Upadhyay, S. Gill and M. Sihag, Flax and flaxseed oil: an ancient medicine and modern functional food, *J. Food Sci. Technol.*, 2014, **51**, 1633–1653.
- S. Melchior, S. Calligaris, G. Bisson and L. Manzocco, Understanding the impact of moderate-intensity pulsed electric fields (MIPEF) on structural and functional characteristics of pea, rice and gluten concentrates, *Food Bioprocess Technol.*, 2020, **13**, 2145–2155.
- A. Brodkorb, *et al.*, INFOGEST static in vitro simulation of gastrointestinal food digestion, *Nat. Protoc.*, 2019, **14**, 991–1014.
- S. Gallier, K. C. Gordon and H. Singh, Chemical and structural characterisation of almond oil bodies and bovine milk fat globules, *Food Chem.*, 2012, **132**, 1996–2006.
- U. K. Laemmli, Cleavage of structural proteins during the assembly of the head of bacteriophage T4, *Nature*, 1970, **227**, 680–685.
- P. K. Smith, *et al.*, Measurement of protein using bicinchoinic acid, *Anal. Biochem.*, 1985, **150**, 76–85.
- K. J. Wiechelman, R. D. Braun and J. D. Fitzpatrick, Investigation of the bicinchoinic acid protein assay: identification of the groups responsible for color formation, *Anal. Biochem.*, 1988, **175**, 231–237.
- D. J. L. Mat, S. Le Feunteun, C. Michon and I. Souchon, In vitro digestion of foods using pH-stat and the INFOGEST



- protocol: Impact of matrix structure on digestion kinetics of macronutrients, proteins and lipids, *Food Res. Int.*, 2016, **88**, 226–233.
- 25 M. C. Carey, D. M. Small and C. M. Bliss, Lipid digestion and absorption, *Annu. Rev. Physiol.*, 1983, **45**, 651–677.
- 26 F. F. Costa, *et al.*, Microfluidic chip electrophoresis investigation of major milk proteins: study of buffer effects and quantitative approaching, *Anal. Methods*, 2014, **6**, 1666–1673.
- 27 R. Sousa, R. Portmann, S. Dubois, I. Recio and L. Egger, Protein digestion of different protein sources using the INFOGEST static digestion model, *Food Res. Int.*, 2020, **130**, 108996.
- 28 A. MacIerzanka, *et al.*, The effect of gel structure on the kinetics of simulated gastrointestinal digestion of bovine  $\beta$ -lactoglobulin, *Food Chem.*, 2012, **134**, 2156–2163.
- 29 L. Manzocco, *et al.*, Structural characterisation and sorption capability of whey protein aerogels obtained by freeze-drying or supercritical drying, *Food Hydrocolloids*, 2022, **122**, 107117.
- 30 M. G. Ferruzzi, The influence of beverage composition on delivery of phenolic compounds from coffee and tea, *Physiol. Behav.*, 2010, **100**, 33–41.
- 31 F. Valoppi, *et al.*, Influence of oil type on formation, structure, thermal, and physical properties of monoglyceride-based organogel, *Eur. J. Lipid Sci. Technol.*, 2017, **119**, 1500549.
- 32 A. de Vries, Y. L. Gomez, E. van der Linden and E. Scholten, The effect of oil type on network formation by protein aggregates into oleogels, *RSC Adv.*, 2017, **7**, 11803–11812.
- 33 Y. Li and D. J. McClements, New mathematical model for interpreting pH-stat digestion profiles: Impact of lipid droplet characteristics on in vitro digestibility, *J. Agric. Food Chem.*, 2010, **58**, 8085–8092.
- 34 E. J. Campbell, Sunflower oil, *J. Am. Oil Chem. Soc.*, 1983, **60**, 387–392.
- 35 A. Ashkar, S. Laufer, J. Rosen-Kligvasser, U. Lesmes and M. Davidovich-Pinhas, Impact of different oil gelators and oleogelation mechanisms on digestive lipolysis of canola oil oleogels, *Food Hydrocolloids*, 2019, **97**, 105218.
- 36 J. Li, C. Zhang, Y. Li and H. Zhang, Fabrication of aerogel-templated oleogels from alginate-gelatin conjugates for in vitro digestion, *Carbohydr. Polym.*, 2022, **291**, 119603.
- 37 L. Dong, *et al.*, In vitro gastrointestinal digestibility of phytosterol oleogels: Influence of self-assembled microstructures on emulsification efficiency and lipase activity, *Food Funct.*, 2020, **11**, 9503–9513.
- 38 P. Reis, *et al.*, Competition between lipases and monoglycerides at interfaces, *Langmuir*, 2008, **24**, 7400–7407.
- 39 L. Salvia-Trujillo, *et al.*, Lipid digestion, micelle formation and carotenoid bioaccessibility kinetics: Influence of emulsion droplet size, *Food Chem.*, 2017, **229**, 653–662.
- 40 L. Salvia-Trujillo, C. Qian, O. Martín-Belloso and D. J. McClements, Influence of particle size on lipid digestion and  $\beta$ -carotene bioaccessibility in emulsions and nanoemulsions, *Food Chem.*, 2013, **141**, 1472–1480.
- 41 H. Singh, A. Ye and D. Horne, Structuring food emulsions in the gastrointestinal tract to modify lipid digestion, *Prog. Lipid Res.*, 2009, **48**, 92–100.

